Fibers and Polymers 2018, Vol.19, No.9, 1806-1812
DOI 10.1007/s12221-018-7747-5

ISSN 1229-9197 (print version)
ISSN 1875-0052 (electronic version)

Reduced Pressure Curing on Polycarbosilane Precursor for Synthesis of Silicon Carbide Fiber

Young Jun Joo[1], Khos-Erdene Khishigbayar[1]*, Kwang Youn Cho[1]*, and Cheol Jin Kim[2]

[1]*Ceramic Fiber and Composite Materials Center, Korea Institute of Ceramic Engineering and Technology, Jinju 52851, Korea*
[2]*Department of Ceramic Engineering, Gyeongsang National University, Jinju 52828, Korea*

(Received August 31, 2017; Revised June 2, 2018; Accepted July 6, 2018)

Abstract: Low pressure curing method with iodine vapor was used on low softening temperature polycarbosilane (PCS) precursor for fabrication of continuous SiC fiber at relatively low temperature. The low curing temperature can provide with a wide range of softening temperature PCS precursors, especially with low softening PCSs, which have a good spinnability, but many difficulties with conventional oxidation curing method. The low pressure curing method having the presence of iodine vapor have shown the more positive effect on pyrolysis with early stage crystallization of β-SiC at 1300 °C. Crystal size of β-SiC, cured at 0.008 kPa is around 2-3 nm larger than cured at 101 kPa. In addition, the higher tensile strength of SiC fiber at elevated temperature can be obtained at 0.008 kPa with a value of 2.1 GPa, compare to 1.3 GPa at 101 kPa of curing pressure condition.

Keywords: Iodine vapor curing, Silicon carbide fiber, Polycarbosilane, Low pressure curing

Introduction

The demand of silicon carbide fibers with excellent mechanical properties and lower price have been challenged in a long period, and it has been an ultimate motivation in this research area [1,2]. High-performance SiC fibers were successfully obtained from polycarbosilane (PCS) precursor polymer with conventional thermal oxidation curing method at low temperature [3,4].

However, the presence of oxygen in the fiber causes high-temperature instability; it is incorporated with thermal degradation and carbothermal reduction [5]. Thermo-mechanical degradation of SiC fibers mentioned in earlier works, and it highly depends on its application atmosphere. However, a considerable amount of weight losses can occur at a temperature as low as 1100 °C and tensile strength reduction can start with the temperatures below 900 °C [6]. Literature has suggested that these effects are originated with the presence of oxygen (8-15 wt.%) and excess carbon in fibers [7,8]. The presence of these elements leads to the evolution of volatile species, which results in some degree of weight losses in the fiber body. Therefore, thermo-mechanical degradation occurred due to the formation of porosity and growth of SiC grains, those forced to the defects in the fiber microstructure [9].

Many scientists reported non-oxidation curing methods on PCS precursor such as electron beam radiation [10], UV assisted radiation [11], cyclohexane vapor curing [12], unsaturated hydrocarbon vapor [5,13] and so on. In addition, many studies attempted to obtain SiC fiber from oxygen-free sources and using some additives with PCS [14,15].

One of those methods, our previous work suggested that iodine vapor curing can avoid disadvantages mentioned above related to the oxygen content in the fiber [16]. The iodine vapor curing method can provide an excellent curing effect on the wide range of PCS precursor at comparatively low temperatures in the various curing atmosphere [17,18]. In this work, we have improved the performance of previously discussed iodine vapor curing method with lower curing pressure. We have found that low pressure curing atmosphere has advantages over the other curing atmospheres (air, nitrogen, and argon), especially with iodine vapor penetration degree into fiber's core. In this study, the PCS fiber curing process performed with a ratio of sample and iodine at 1:1 under low pressure condition and results were summarized with appropriate methods.

Experimental

Raw Material

Commercially available PCS (TBMTech Co. Ltd., Korea) was used as a precursor for fabrication of SiC fiber. The characteristics of the PCS precursor summarized in Table 1. Pure elemental iodine, ACS grade (Daejung Chemicals Co. Ltd., Korea) was used as the doping element.

Fabrication of SiC Fiber

PCS powder was melted at 150 °C for 1 h in a vacuum due to the evaporation of the toluene, which carried into PCS during its manufacturing process and stabilized at 190 °C for 2 hs with the low vacuum condition in a single-hole spinneret. Melt-spinning proceeded at 190-200 °C under 0.01-0.05 MPa pressure with 10 rpm of winding speed. The diameter of spun fiber was 10-15 μm. Subsequently, PCS spun fiber cured in the vacuum chamber with the presence of iodine vapor at a various pressure; 0.008 kPa, 0.08 kPa, 0.8 kPa and 101 kPa at 150 °C for 2 hs. Nitrogen was employed as an

---

*Corresponding author: jose2010@naver.com
*Corresponding author: kycho@kicet.re.kr

Table 1. Characteristics of as-received PCS precursor

Mn (Daltons)	Mw (Daltons)	MP (Daltons)	Mz (Daltons)	Mz+1 (Daltons)	Polydispersity	a t_S (°C)	b t_m (°C)
2574	5210	3857	10630	18023	2.02	140	175

[a]Softening temperature of PCS precursor and [b]melting temperature of PCS precursor.

atmosphere gas when using atmospheric pressure for curing. During the curing process, same volume of crucible was used along with constant amount of PCS fiber and iodine. The curing ratio of PCS fiber to iodine was 1:1. Subsequently, the cured fibers were pyrolized at 1300 °C with 10 °C of the heating rate for 1 h in graphite furnace under an argon atmosphere.

Measurements

The softening and melting point of the PCS precursor was measured with melting point instrument digital apparatus (IA9100, Bibby Scientific Co. Ltd., USA). Small crystal sized PCS placed into capillary tube and it was sealed with vacuum in order to measure softening and melting point. Fast ramp rate of 10 °C/min used in the beginning and it was slowed down at 1 °C/min at near softening zone. The average molecular weight was determined by gel permeation chromatography system equipped with Waters 515 HPLC pump, a Waters 2414 refractive index detector. Toluene was used as a solvent, and the flow rate was 1 m*l*/min. Calibration was performed using polystyrene standards for the accuracy and precision of equipment.

The chemical structure of as-received PCS and the structural modification of the cured PCS fibers measured with Fourier transform infrared spectroscopy (FT-IR) analysis equipment (FT/IR-4100, JASCO, Japan) in high purity nitrogen environment. The samples were incorporated into potassium bromide pellets. The morphological studies of PCS precursor, the cured PCS fibers and fabricated SiC fibers performed by FE-SEM (JSM-7610F, JEOL, Japan) and EDS analysis (X-MAX 50, OXFORD, England). Thermogravimetric analysis has been employed to determine the ceramic yields of starting material and the cured PCS fibers up to 1000 °C with 10 °C/min of heating rate while using nitrogen atmosphere (DTG-60H, Shimadzu, Japan). Analysis of phase composition of fabricated SiC fibers was performed by X-ray diffraction (DMAX 2500, Rigaku, Japan), using Cu Kα irradiation (2θ=10 °-80 °). Crystallization degree of experimental products was measured by 400kV TEM (JEM-4010, JEOL, Japan) analysis, performed to optimize the fiber fabrication conditions. Also, elevated temperature tensile strength of heat-treated SiC fibers determined at 1200 °C in air. A self-induced tensile strength measurement system (load cell: UMI-G200, DACELL, Korea) was used for SiC fiber mechanical strength measurements, in which SiC fibers for each testing condition were attached to a test sheet and pulled at the speed of 0.5 mm/min.

Results and Discussion

Figure 1 and Table 1 show some basic characteristics of PCS (TBMTech) precursor such as molecular weight information, softening and melting temperatures. The number average molecular weight (Mn) and a weight average molecular weight (Mw) were 2574 and 5210, respectively. The polydispersity (Mw/Mn) of PCS precursor was 2.02.

Melt spun, and the cured PCS fibers were studied by FT-IR analysis in a range of 400-4000 cm^{-1} and it shows that the low-temperature curing on the PCS fibers with iodine at low pressure has a potential as its high-temperature curing (Figure 2). The iodine was playing an important role for cross-linking of PCS precursor fibers under the low pressure environment.

According to FTIR analysis, Si-H stretching (2100 cm^{-1}) decreased, while enhancement of Si-CH$_2$-Si stretching (1020 cm^{-1} and 1355 cm^{-1}) observed in the spectrum due to differences in curing pressure used for the curing process.

In particular, the degree of Si-H cleavage decreased along with the reduction of curing pressure. The iodine vapor curing causes degradation of particular groups in the PCS molecules, such as -CH$_3$, thus causes to form reactive sites, which are playing a critical role for further cross-linking [18]. Also, this dehydrogenation processes lead to the formation of C=C bonds in the PCS structure [16]. However, the occurrences of C=C bonds (1540 ADScm^{-1} and 1630 cm^{-1}) increased at higher pressure curing. It confirmed that not the all C-H cleavage was leading to develop C=C bonds at the lower pressure curing, despite the greater degree of C-H

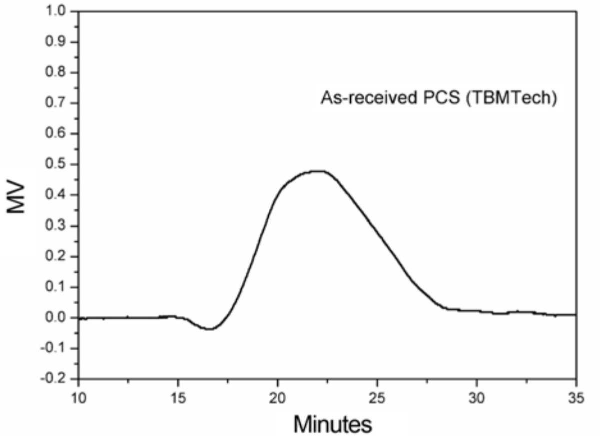

Figure 1. Gel permeation chromatogram of as-received PCS precursor.

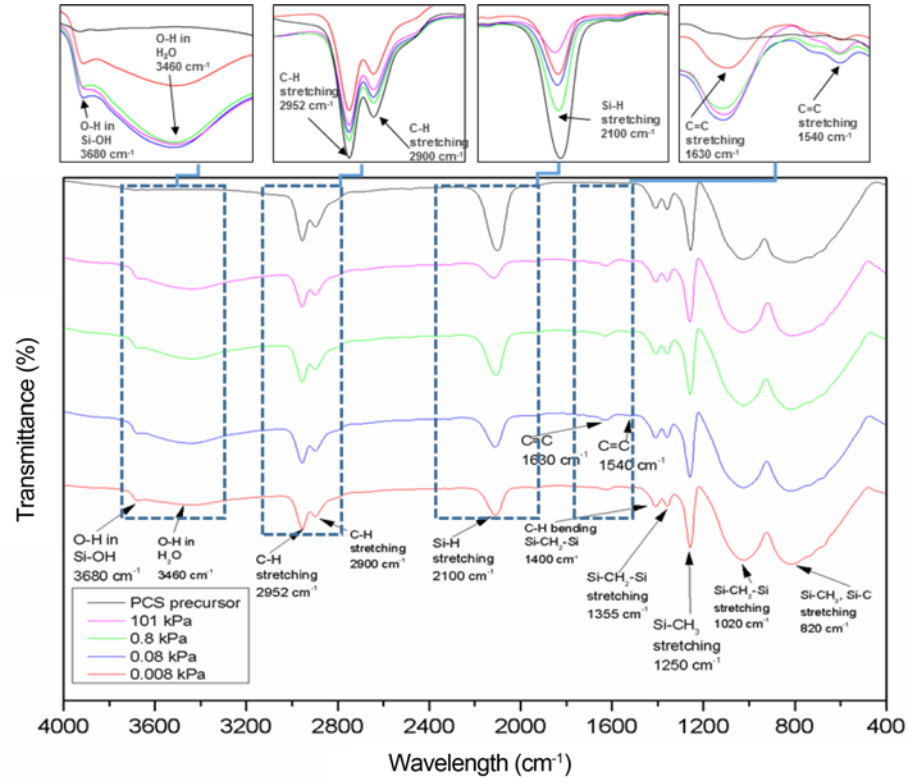

Figure 2. FT-IR spectra of as-spun PCS, PCS fibers cured at low pressure (0.8 kPa, 0.08 kPa and 0.008 kPa), PCS fiber cured at atmospheric pressure (101 kPa).

cleavage than the atmospheric pressure curing. Otherwise, the lower pressure curing lead into formation of more reactive sites rather than the establishment of C=C bonds. The heat resistance of fiber is related to increased peaks such as $Si-CH_2-Si$ and $Si-CH_3$ stretching [19]. Iodine played a key role in breaking Si-H and C-H bond and then, to induce for the development of Si-C-Si linkage in curing products. However, O-H stretching in Si-OH and H_2O (3460 cm^{-1} and 3680 cm^{-1}) newly appeared with FT-IR analysis; it strongly related to absorption behavior between iodine and water.

Ly *et al.* suggest that the formation of water indicated by the appearance of the band at 3460 cm^{-1} could be due to the reaction [20]:

$$2Si-H + O_2 \rightarrow 2Si-OH \rightarrow Si-O-Si + H_2O$$

However, we proceeded the curing at low pressure, above mentioned reaction could not occur in the cured fiber. Since the iodine is the main component of the cured fiber surface, it can easily absorb water from the air as much as in a short period. Figure 3 shows the exposing rate of cured PCS fiber in the air after the curing. Therefore, the very short time needed to transfer cured sample from the curing chamber to heat treatment furnace. Also, water molecules could be introduced to the cured fibers during the sample preparation for analysis.

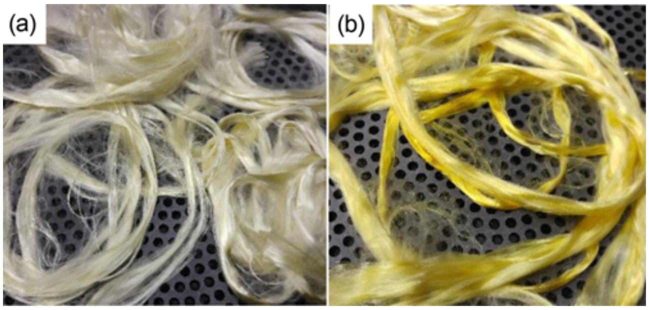

Figure 3. PCS fibers cured at low pressure (PCS 1:1 iodine); (a) cured PCS fiber after 10 sec in air and (b) cured PCS fiber after 3 min in air.

Figure 4 indicates the results of the thermogravimetric analysis for as-received PCS and the cured PCS fibers, respectively. The ceramic yield of all the cured fibers increased significantly compared to the as-received PCS. As shown in Figure 4, the significant amount of weight loss for as-received PCS fiber started at 250 °C. It is considered to relate with low molecular weight fractions, which have low melting temperatures. On the other hand, the weight decrease of all the iodine vapor cured PCSs started below 100 °C. Since all the cured fibers contain more than 10 % of the iodine in their body, the introduced volatile iodine evaporation would start from the surface at a temperature below 100 °C.

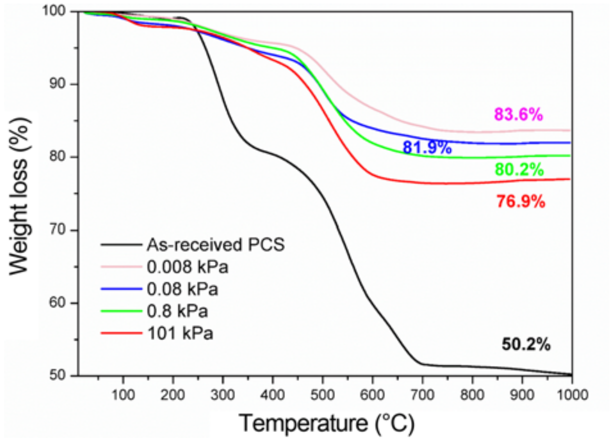

Figure 4. TG curves of un-cured and cured PCS fibers at 0.008 kPa, 0.08 kPa, 0.8 kPa and 101 kPa.

The weight change pattern of these cured samples above 200 °C was almost the same as that of ac-received PCS fiber; it is considered degradation of low molecular weight molecules or decomposition of organic side groups [21]. However, the increase of ceramic yield by iodine vapor curing was obtained from these all the cured samples. The values of weight loss difference between as-received and iodine vapor cured PCSs were around 26-33 % depending on curing pressure. As mentioned in the FT-IR results, it is considered that the cleavage of C-H and Si-H increased along with decreased curing pressure, which is leading to cross-linking with reactive sites in the PCS fibers. This phenomenon confirmed with the results of TG analysis; the increase of ceramic yield along with decreased curing pressure.

The ceramic yield of PCS strongly depends on the degree of cross-linking of the polymer. Therefore, results of FT-IR and TG analysis showed that the degree of cross-linking in the PCS was increased significantly at lower pressure curing than atmospheric pressure curing.

It is a critical to explain on curing mechanism between PCS and iodine during the low pressure curing, due to this purpose, SEM and EDS analysis have been used to determine the distribution of each element at surface and core of the cured fibers (Figure 5 and Figure 6). In the case of SEM analysis, the morphology of SiC fibers have not shown apparent differences (not shown in this paper).

According to EDS line profile analysis, a higher degree of iodine diffusion was observed at the surface than its core with higher curing pressure at 0.08 kPa, 0.8 kPa, and 101 kPa. On the other hand, the almost constant amount of iodine diffusion degree was observed at surface and core of the fibers with lower curing pressure at 0.008 kPa. Iodine molecules can penetrate deeply to the fiber core at the low pressure curing than the atmospheric pressure curing. Iodine diffusion into fiber core can make better cross-linking for the further high-temperature application. It is considered that the mean free path is increased drastically in vacuum, meaning a single particle of iodine molecule travels long distances, possibly ending up hitting the PCS fiber surface instead of frequently hitting each other. As a result, it may lead more deep diffusion of iodine molecules into fiber core.

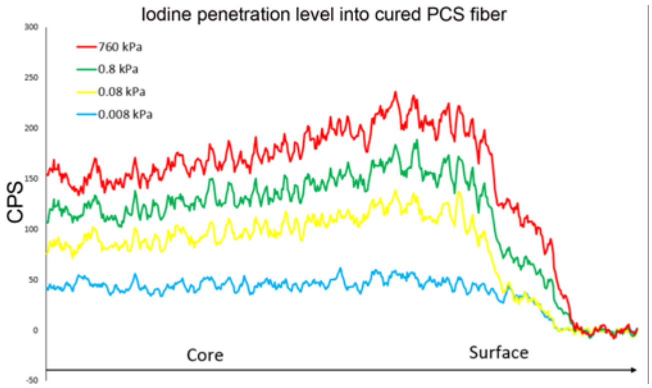

Figure 5. Elemental EDS line profiles on iodine distribution for cross-section of PCS fibers cured at 0.008 kPa, 0.08 kPa, 0.8 kPa and 101 kPa.

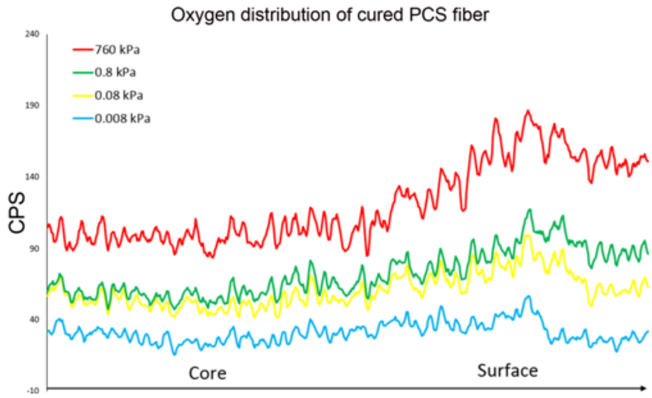

Figure 6. Elemental EDS line profiles on oxygen distribution for cross-section of PCS fibers cured at 0.008 kPa, 0.08 kPa, 0.8 kPa and 101 kPa.

For oxygen content, an identical tendency with the distribution of iodine was observed in the all cured PCS fibers (Figure 6). The weight percent of oxygen was much higher with atmospheric pressure curing, although high purity nitrogen was used as an inert atmosphere. Clearly, the amount of oxygen weight percentage at surface was greater than its core, except 0.008 kPa of curing pressure which has shown the steady amount of weight percentage at core and surface.

Figure 7 and Figure 8 represents the detailed structural analysis of fabricated SiC fibers carried out by TEM. The microstructure of fabricated SiC fibers was changed remarkably by the iodine vapor curing at low pressure. According to TEM, the crystal size of SiC fiber cured at 101 kPa and

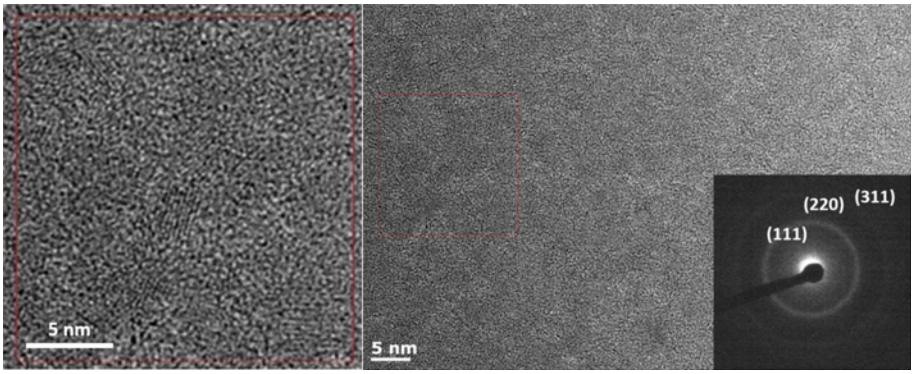

Figure 7. TEM analysis of fabricated SiC fiber; fabricated by iodine-vapor curing at 101 kPa.

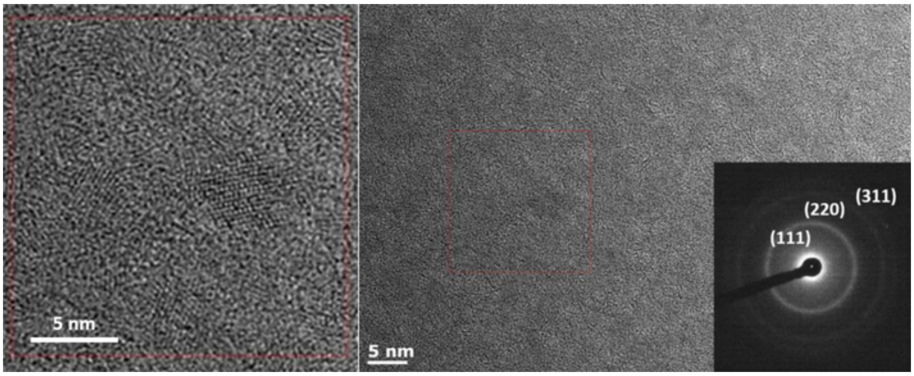

Figure 8. TEM analysis of obtained SiC fiber; fabricated by iodine-vapor curing at 0.008 kPa.

0.008 kPa were 1-3 nm and 3-5 nm, respectively. It proved that the low pressure curing (0.008 kPa) have a positive effect on the crystallization degree of the final product. Therefore, considering the results shown in FT-IR (Figure 2), TG (Figure 4) and TEM analysis (Figure 7 and Figure 8), the iodine vapor curing at low pressure is more efficient for further fabrication of SiC fiber.

The X-ray diffraction pattern of the fabricated SiC fibers in Figure 9 shows the amorphous nature of β-SiC phase due to relatively broad peaks compared with standard XRD pattern. All of the fabricated fibers have shown similar peaks which were assigned to the (PDF No. 29-1129) (111) ($2\theta=35.6^{\circ}$; d=0.251 nm), (220) ($2\theta=60^{\circ}$; 2d=0.154 nm) and (311) ($2\theta=71.8^{\circ}$; 2d=0.131 nm) planes of β-SiC [22,23], despite the different curing condition. The three main peaks are sharpened along with decreased curing pressure shows that crystallization degree of β-SiC was greater at low pressure than atmospheric curing. The early stage crystallization of β-SiC avoids oxygen uptake into the fibers. A typical amorphous SiOC phase observed at $2\theta=20\text{-}22^{\circ}$ in the atmospheric pressure (101 kPa) cured sample. The presence of the SiOC phase meant that the crystallization and growth of β-SiC are delayed even at 1300 °C [22]. Also, silicon oxycarbides lead into low heat resistance for the fiber in the high-temperature application.

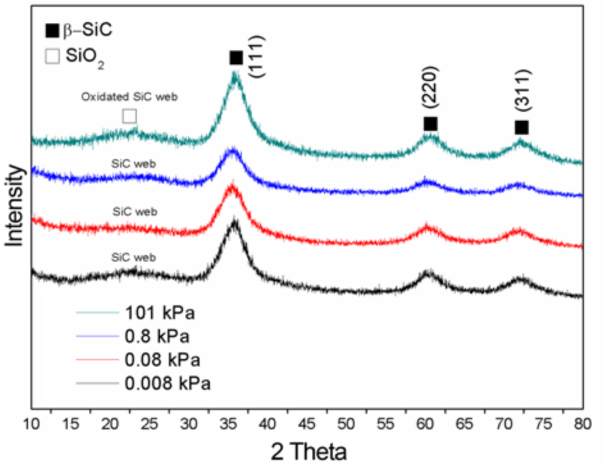

Figure 9. XRD patterns of pyrolized (at 1300 °C) SiC fibers; fabricated by iodine-vapor curing at 0.008 kPa, 0.08 kPa, 0.8 kPa and 101 kPa.

Figure 10 indicates stress-strain curves of the fabricated SiC fibers cured at various curing pressure, along with their average tensile strength at 1200 °C. The average tensile strength was found 1.3 GPa, 1.5 GPa, 1.6 GPa and 2.1 GPa at 101 kPa, 0.8 kPa, 0.08 kPa and 0.008 kPa, respectively.

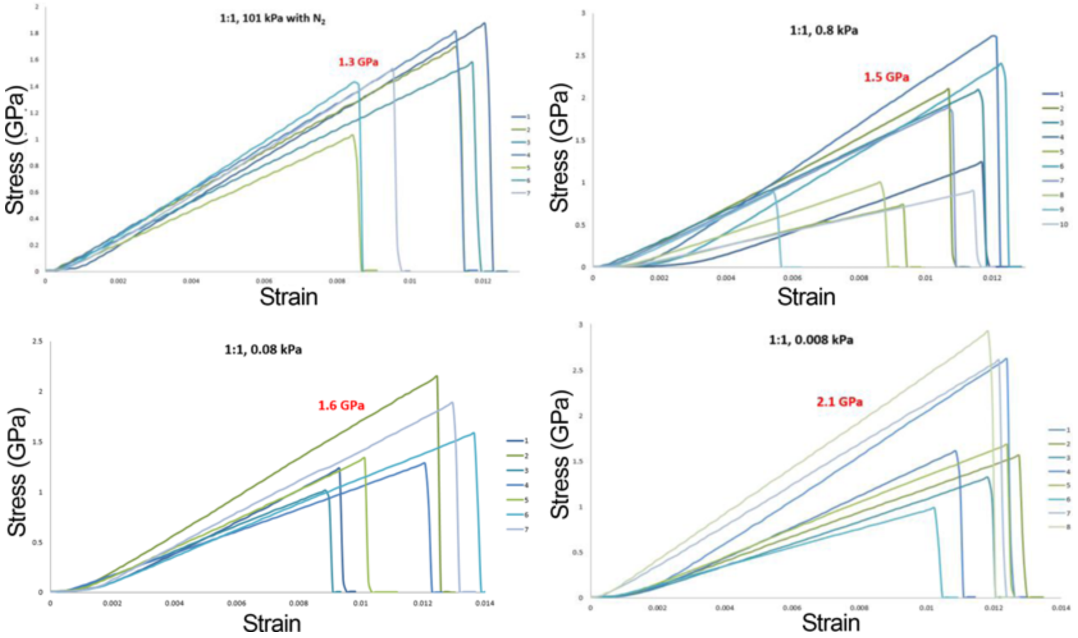

Figure 10. Stress-strain curve of obtained SiC fibers; fabricated by iodine-vapor curing at 0.008 kPa, 0.08 kPa, 0.8 kPa and 101 kPa.

Also, tensile elastic modulus of each fiber has been calculated from the stress-strain curve with values of 136 GPa, 160 GPa, 172 GPa and 184 GPa at previously mentioned curing conditions.

The tensile strength of SiC fiber decreases in the high temperature as a result of β-SiC grain growth which cause larger flaw sizes in the fiber structure [24,25]. Hence, we controlled the grain size of the β-SiC crystal under 5 nm up to 1300 ^{o}C of heat treatment temperature in order to hinder excessive crystallization process. Also, oxygen content in the heat treated SiC fiber can play an important role for its tensile strength due to degradation process at high temperature [26]. The results of tensile strength were well matched with the other analysis due to lower cross-linking and higher oxygen content in the fiber lead for degradation at the elevated temperature.

Conclusion

High-performance silicon carbide fibers were successfully obtained from low softening temperature PCS with the presence of iodine using low pressure curing at 0.008 kPa. The iodine molecules distributed uniformly into PCS fiber during the curing at lower pressure than higher pressure. An elevated temperature performance of obtained SiC fibers from low softening point PCS are comparatively high as well as their high softening point PCS precursor. The low pressure curing leads production and crystallization of β-SiC at a shorter period than required if cured at atmospheric pressure. Additionally, the low pressure cured SiC fibers contained comparatively small amount of oxygen and it results to delay the degradation process of SiC fibers at elevated temperature.

Acknowledgements

The authors are appreciative for the financial support from the Korean Ministry of Knowledge and Economy, and the “Ceramic Fiber Commercialization Center” within the Korea Institute of Ceramic Engineering and Technology.

References

1. A. R. Bunsell and A. Piant, *J. Mater. Sci.*, **41**, 823 (2006).
2. H. J. Hwang, K. J. Lee, Y. T. An, B. H. Choi, and W. S. Seo, *Mater. Chem. Phys.*, **134**, 13 (2012).
3. P. Colombo, G. Mera, R. Riedel, and G. D. Sorarù, *J. Am. Ceram. Soc.*, **93**, 1805 (2010).
4. H. Wang, X. D. Li, X. X. Li, B. Zhu, and D. P. Kim, *Korean J. Chem. Eng.*, **21**, 901 (2004).
5. Y. Hasegawa, *Compos. Sci. Technol.*, **51**, 161 (1994).
6. W. Toreki, C. D. Batich, M. D. Sacks, M. Saleem, G. J. Choi, and A. A. Morrone, *Compos. Sci. Technol.*, **51**, 145 (1994).
7. M. D. Sacks, *J. Eur. Ceram. Soc.*, **19**, 2305 (1999).
8. A. Otsuka, Y. Matsumura, K. Hosono, and R. Tanaka, *J. Eur. Ceram. Soc.*, **23**, 3125 (2003).
9. M. Takeda, A. Urano, J. Sakamoto, and Y. Imai, *J. Nucl. Mater.*, **258-263**, 1594 (1998).
10. Z. Su, L. Zhang, Y. Li, S. Li, and L. Chen, *Am. Ceram. Soc.*, **98**, 2014 (2015).
11. H. Li, L. Zhang, L. Cheng, H. Kang, and Y. Wang, *J.*

Mater. Sci., **44**, 970 (2009).
12. W. Li, Y. C. Song, and X. H. Mao, *J. Mater. Sci*., **41**, 7011 (2006).
13. Y. Hasegawa, *J. Inorg. Organomet. Polym.*, **2**, 161 (1992).
14. Z. Xie and Y. Gou, *Ceram. Int.*, **42**, 10439 (2016).
15. Z. Su, M. Tang, Z. Wang, L. Zhang, and L. Cheng, *J. Am. Ceram. Soc*., **93**, 679 (2010).
16. J. Hong, K. Y. Cho, D. G. Shin, J. I. Kim, S. T. Oh, and D. H. Riu, *J. Mater. Chem. A*., **2**, 2781 (2014).
17. Hong, K. Y. Cho, D. G. Shin, J. I. Kim, and D. H. Riu, *J. Appl. Polym. Sci*., **132**, 42687 (2015).
18. J. Hong, K. Y. Cho, D. G. Shin, J. I. Kim, and D. H. Riu, *RSC Adv.*, **5**, 83847 (2015).
19. R. K. Gupta, R. Mishra, R. K. Tiwari, A. Ranjan, and A. K. Sahena, *Silicon*, **3**, 27 (2011).
20. H. Q. Ly, R. Taylor, R. J. Day, and F. Heatley, *J. Mater. Sci.*, **36**, 4037 (2001).
21. Y. Hasegawa, M. Iimura, and S. Yajima, *J. Mater. Sci*., **15**, 720 (1980).
22. H. Q. Ly, R. Taylor, R. J. Day, and F. Heatley, *J. Mater. Sci*., **36**, 4045 (2001).
23. J. J. Sha, J. S. Park, T. Hinoki, and A. Kohyama, *Mater. Charact*., **57**, 6 (2006).
24. J. J. Sha, T. Nozawa, J. S. Park, and Y. Katoh, *J. Nucl. Mater*., **329-333**, 592 (2004).
25. R. Q. Yao, Y. Y. Wang, and Z. D. Feng, *Fatigue. Fract. Eng. Mater. Struct*., **31**, 777 (2008).
26. K. E. Kim, K. Khishigbayar, and K. Y. Cho, *J. Adv. Ceram*., **6**, 59 (2017).